

Research Article

In Vitro Cytotoxicity Assay on Gold Nanoparticles with Different Stabilizing Agents

S. Vijayakumar¹ and S. Ganesan²

¹Department of Physics, Sri Ramakrishna Institute of Technology, Pachapalayam, Peruruchettipalayam, Coimbatore 641010, India

²Department of Physics, Government College of Technology, Thadagam Road, Coimbatore 641013, India

Correspondence should be addressed to S. Vijayakumar, vijaysk.research@gmail.com

Received 9 April 2012; Revised 16 July 2012; Accepted 20 July 2012

Academic Editor: Xiaoming Li

Copyright © 2012 S. Vijayakumar and S. Ganesan. This is an open access article distributed under the Creative Commons Attribution License, which permits unrestricted use, distribution, and reproduction in any medium, provided the original work is properly cited.

Noble gold nanoparticles (AuNps) are generally nontoxic due to their inert nature. The gold nanoparticles are easily tagged with various proteins and biomolecules rich in aminoacid leading to important biomedical applications including targeted drug delivery, cellular imaging, and biosensing. In this study, three cytotoxicity detection assays 3-(4,5-dimethylthiazol-2-yl)-2,5-diphenyl tetrazolium bromide (MTT), neutral red cell, and lactate dehydrogenase (LDH) on gold nanoparticles stabilized with citrate, starch, and gum arabic are used. The assays used are based on different mode of detection like LDH release, MTT metabolism, and neutral red uptake. We found that the AuNps stabilized with citrate are very sensitive to the change of concentration and time assay compared to starch and gum arabic stabilized gold nanoparticles.

1. Introduction

Gold nanoparticles possess different physiochemical characteristics compared to the bulk gold [1, 2]. The six free electrons present in the conduction band of gold nanoparticles make them a potential candidate to bind with thiols and amines [3], also gold nanoparticles easily tagged with various proteins and biomolecules rich in aminoacids leading to important biomedical applications including targeted drug delivery [4, 5], cellular imaging [6], and biosensing [7]. The use of nanoparticles for biomedical applications such as drug and gene delivery, biosensors, cancer treatment, and diagnostic tools has been extensively studied throughout the past decade [8–17].

The toxicity has been expected to be in the following strategy [18]. The toxic CdSe can release poisonous cadmium ions inside the living organism and by competing with zinc for binding sites on metallothionein [19]. The nanoparticles have been shown to adhere to cell membranes [20] and also be ingested by cells [21]. The breaching of the cell membrane and the intracellular storage may have a negative effect on the cells regardless of the toxicity of the particles and their subsequent functionality.

Microstructure is essential for inductive bone formation in calcium phosphate materials after soft-tissue implantation. The increasing surface areas, microstructured calcium phosphate materials might concentrate more proteins that differentiate inducible cells from osteogenic cells that form inductive bone [22]. The multiwalled carbon nanotubes (MWNTs) might stimulate inducible cells in soft tissues to form inductive bone by concentrating more proteins, including bone-inducing proteins [23]. Distinctly shaped nanoparticles such as carbon nanotubes can rip cells like needle [24]. This suggests that nanomaterials of the same composition would have different biologic responses for different morphologies. The advantages of the *in vitro* approach includes simplicity, consistency of the experimental setup, and the reproducibility of the experimental results [25].

Cytotoxicity also depends on the type of cells used. The 33 nm citrate-capped gold nanoparticles were found to be nontoxic to baby hamster kidney and human hepatocellular liver carcinoma cells but toxic to a human carcinoma lung cell lines. AuNps may have advantages over other metallic nanoparticles in terms of biocompatibility and noncytotoxicity [26].

In this study, gold nanoparticles stabilized with citrate, starch, and gum arabic are used for cytotoxicity studies. The assays used are based on different modes of detection like LDH release, MTT metabolism, and Neutral Red uptake. We found some noticeable differences in the values for the cytotoxic effect depending on the assay and nanoparticle capping agent used. In particular, the citrate stabilized gold nanoparticles are having little toxicity compared to the starch and gum arabic stabilized nanoparticles, since we have used the same size of particles in all the cases.

2. Materials and Methods

All chemicals were obtained from Sigma-Aldrich and used as received. Double-distilled water was used in all experiments. The PC-3 and MCF-7 cell lines were obtained from the American Type Culture Collection (ATCC) through Department of Microbiology, PSG Institute of Medical Sciences and Research, Tamilnadu, India. The cell line (CHO22) was obtained from R&D-Bio, Coimbatore, India.

2.1. Preparation of Gold Nanoparticles

2.1.1. Preparation of Citrate-Capped Gold Nanoparticles (Citrate-AuNps). Conventional techniques for aqueous synthesis of gold nanoparticles involve reduction of Au(III)Cl₃ with trisodium citrate, a process pioneered by Turkevich and later refined by Frens [27–30]. In this method the citrate salt initially acts as a reducing agent by forming a layer of citrate ions over the gold nanoparticles surface, inducing enough electrostatic repulsion between individual particles to keep them well dispersed in the medium. This method provides uniform and fairly spherical nanoparticles.

This reduction process proceeds at a very slow rate and imparts a wine red color to the solution. 250 mL of 0.25 mM HAuCl₄ was heated to boiling. Then, 4 mL of aqueous solution of 1% solution of trisodium citrate was added to the HAuCl₄ solution under vigorous stirring and the boiling was continued for 15 min until it turns to a deep red colour. The citrate ions serve as both reducing agent for AuNp formation and a stabilizer, preventing agglomeration of gold nanoparticles.

2.1.2. Preparation of Starch-Capped Gold Nanoparticles (Starch-AuNps). Starch (0.0225 g) was dissolved in 6 mL of doubly ionized water by heating the solution to 90–100°C with continuous stirring. To this hot starch solution, 0.1 mL of 0.1 M HAuCl₄ solution (0.0393 g in 1 mL deionized water) was added, followed by the addition of 0.02 mL of 0.1 M trialanine phosphine (THPAL) solution (0.0337 g in 1 mL DI water) with continuous stirring. When the color of the solution changed to pinkish purple, stirring was continued for one minute without heating.

2.1.3. Preparation of Gum Arabic-Capped Gold Nanoparticles (Gum Arabic-AuNps). Gum Arabic (0.012 g) was dissolved in 6 mL of doubly ionized water by heating the solution to 90–100°C with continuous stirring. To this hot gum arabic solution, 0.1 mL of 0.1 M NaAuCl₄ solution (0.0338 g

TABLE 1: Average size, plasmon wavelength, and plasmon width of gold nanoparticles stabilized with starch, gum Arabic, and citrate.

Sample name	Average size (nm)	Plasmon wavelength λ_{max} (nm)	Plasmon width $\Delta\lambda$ (nm)
C-AuNp	21 ± 1.4	523	90
S-AuNp	21 ± 1.5	525	90
GA-AuNp	20 ± 2.3	528	85

in 1 mL DI water) was added, followed by the addition of 0.02 mL of 0.1 M THPAL solution (0.0338 g in 1 mL DI water) with continuous stirring (Table 1). When the color of the solution changed to reddish purple, stirring was continued for one minute without heating. Table 2 shows the reaction condition for preparing citrate, starch, and gum arabic stabilized gold nanoparticles.

2.2. Characterization. Gold nanoparticles stabilized with citrate, starch, and gum arabic were characterized by UV-Vis absorption spectroscopy using UV-1700 series spectrometer (PSG Institute of Advanced Studies, Coimbatore, India) to study the peak absorption band. About 1 mL solution of nanoparticles in water was used. The peak absorption band obtained for citrate, starch, and gum arabic stabilized gold nanoparticles is 523 nm, 525 nm, and 528 nm, respectively, (Table 1). TEM images of citrate-, starch- and gum arabic-capped gold nanoparticles were collected on a Philips CM200 (Sophistical Analytical Instrument Facility, Indian Institute of Technology, Bombay, India). The operating voltage range was 20–200 kV with a resolution of 2.4 Å. Zeta potential measurements were performed using a Malvern Instruments Zeta sizer 1000 Hs operating with a variable power (5–50 mW) He-Ne laser at 633 nm (Indian Institute of Science, Bangalore, India). Measurements were taken at 25°C. Before and in between the measurements, the cells were washed with ultrahigh pure water. The AuNp thus, formed were characterized using UV-Vis spectroscopy, Zeta potential, and transmission electron microscopy shown in Figures 1, 2, and 3.

2.3. Cytotoxicity Assay

2.3.1. MTT Assay. Cytotoxicity evaluation of citrate-AuNps, starch-AuNps, and gum arabic-AuNps was performed using MTT assay as described by Mossman [31]. Approximately $1 \times 10^5 \text{ mL}^{-1}$ cells (MCF-7 and PC-3) in their exponential growth phase were seeded in a flat-bottomed 96-well polystyrene coated plate and were incubated for 24 hrs at 37°C in a 5% CO₂ incubator. Series of dilution (20, 50, 80, 110, and 140 µg/mL) of gold nanoparticles in the medium was added to the plate in hexaplets. After 24 hours of incubation, 10 µL of MTT reagent was added to each well and was further incubated for 4 hours. Formazan crystals formed after 4 hours in each well were dissolved in 150 µL of detergent and the plates were read immediately in a microplate reader (BIO-RAD microplate reader-550) at 570 nm. Wells with complete medium, nanoparticles and MTT reagent, without cells were used as blanks. Untreated

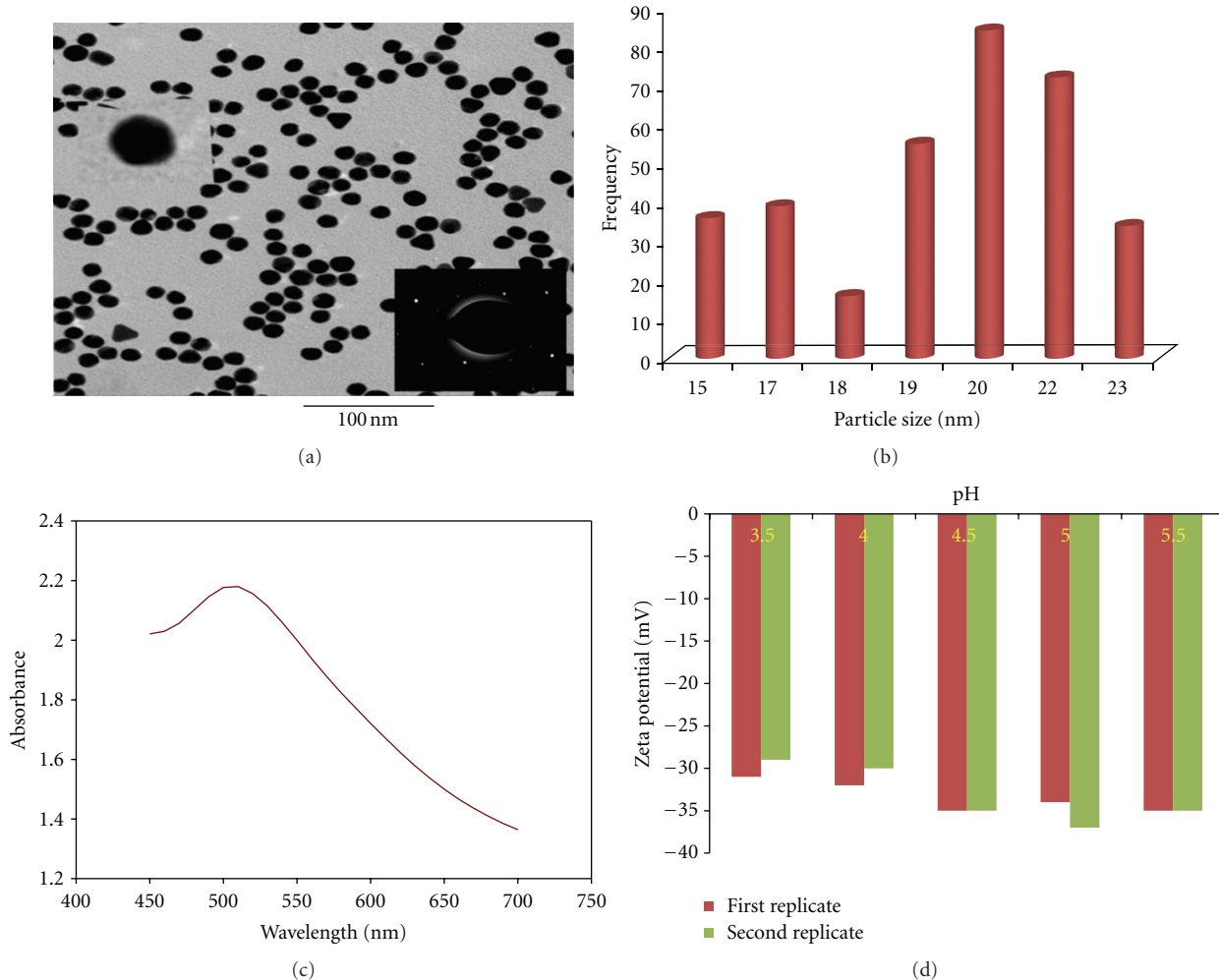


FIGURE 1: (a) TEM image of citrate stabilized gold nanoparticles. Insight SEAD pattern and an enlarged single nanoparticle. (b) Particle size histogram and is 21 nm averaged from 350 nanoparticles. (c) Plasmon resonance absorption and is 523 nm with plasmon width ($\Delta\lambda$) of 90 nm. (d) Zeta potential of gold nanoparticles at different pH values.

TABLE 2: Reaction conditions for producing citrate (C-AuNp), starch (S-AuNp) and gum arabic (GA-AuNp)-capped gold nanoparticles.

Compound name	Stabilizer (C-AuNp)/(S-AuNp)/(GA-AuNp)	Gold precursor	Reducing agent	Time	Reaction solution color
C-AuNp	4 mL of 38.8 mM in 250 mL of DI	0.25 mM HAuCl ₄	4 mL of 1% trisodium citrate	1 min	Wine-red color Sodium citrate
S-AuNp	0.0225 g of starch in 6 mL of DI	0.1 mL of 0.1 M, NaAuCl ₄	0.02 mL of 0.1 M, THPAL	1 min	Pinkish purple
GA-AuNp	0.0225 g of gum arabic in 6 mL of DI	0.1 mL of 0.1 M, NaAuCl ₄	0.02 mL of 0.1 M, THPAL	1 min	Reddish purple

PC-3 and MCF-7 cells as well as the cell treated with (20, 50, 80, 110, and 140 μ g/mL) concentration of AuNPs for 24 hrs were subjected to the MTT assay for cell viability determination.

2.3.2. Neutral Red Cytotoxicity Assay. CHO22 cells were seeded at a population of 1.5×10^4 cells per well in a 96-well plate. The cells were incubated for 24 hours and reached 80–90% confluence. The spent media were removed and the cells were washed with PBS (0.01 M phosphate

buffer, 0.0027 M KCl and 0.137 M NaCl) and 1 μ L fresh media was added. The media were then replaced with test nanoparticles of (20, 50, 80, 110, and 140 μ g/mL) concentrations mixed with fresh media. The plates were then incubated for 24 hrs at 37° in a humidified incubator with a 5% CO₂ environment. Following the incubation periods, the cells were washed twice with PBS (0.01 M phosphate buffer 0.0027 M KCl and 0.137 M NaCl) and 100 μ L serum-free media containing neutral red (100 μ g/mL) was added to each well and incubated for 2-3 hours.

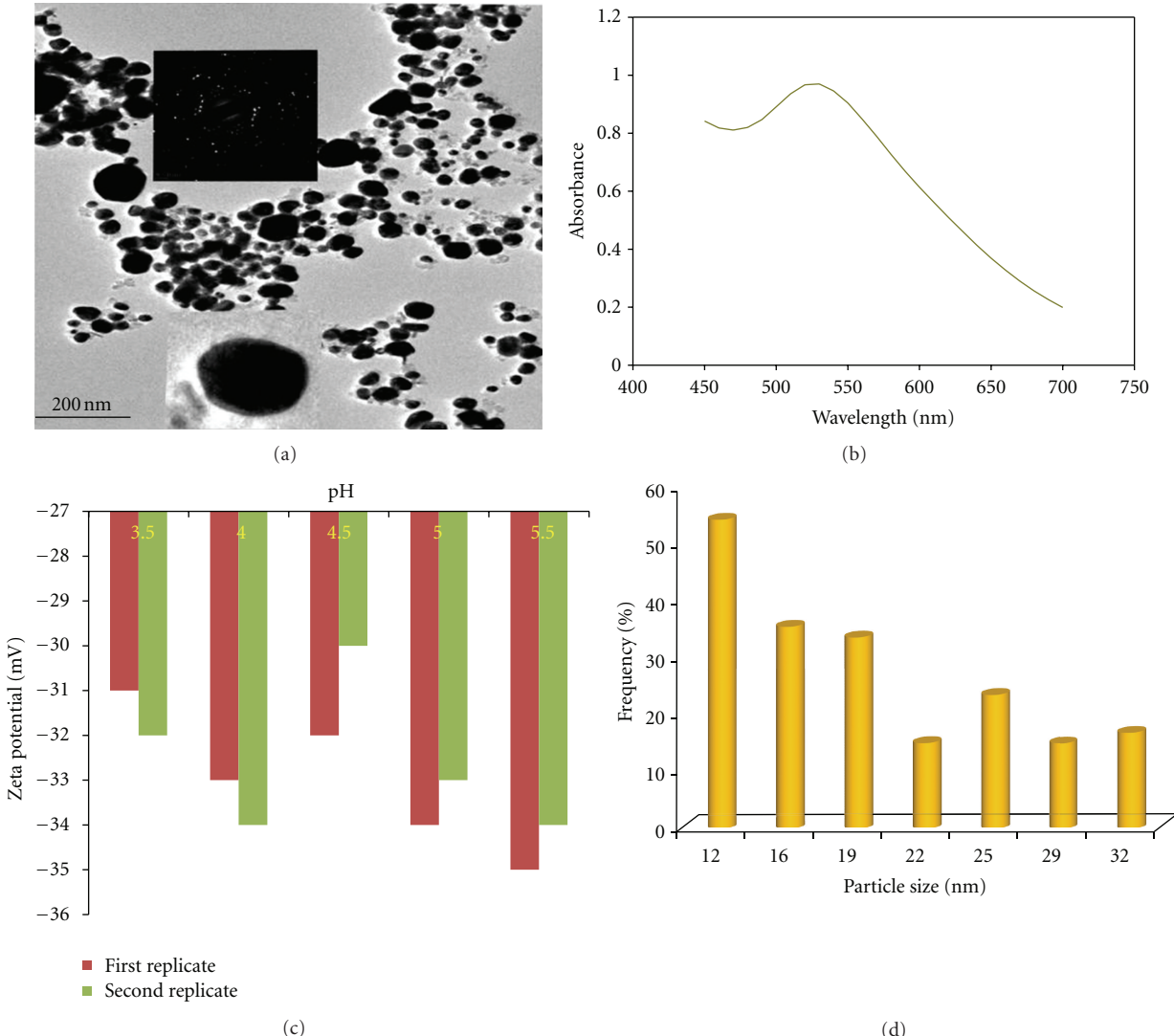


FIGURE 2: (a) TEM image of Starch stabilized gold nanoparticles. Insight SEAD pattern and an enlarged single nanoparticle. (b) Particle size histogram and is 21 nm averaged from 225 nanoparticles. (c) Plasmon resonance absorption and is 525 nm with plasmon width ($\Delta\lambda$) of 90 nm. (d) Zeta potential of gold nanoparticles at different pH values.

After the incubation, the cells were washed twice with PBS (0.01 M phosphate buffer 0.0027 M KCl and 0.137 M NaCl) thereafter 50 μ L of dye release agent (a solution of 1% acetic acid: 50% ethanol) was added to each well and the plates were incubated for further 10 minutes. The plate was placed on a shaker (Vortex Genie) for 30 minutes after which the optical density at 540 nm was determined on a multiwall spectrophotometer.

2.3.3. LDH Assay. Cytotoxicity was assessed using an LDH cytotoxicity detection kit (Roche applied sciences). This assay measures the release of cytoplasm enzyme lactate dehydrogenase (LDH) by damaged cells. Cells cultured in 96 plates were treated with increasing concentrations of gold nanoparticles (20, 50, 80, 110, and 140 μ g/mL). After 48 hours of treatment, culture supernatant was collected and incubated with reaction mixture. The LDH catalyzed

conversion results in the reduction of the tetrazolium salt to formosan, which can be read at 490 nm absorbance. These data are measured in LDH activity as a percentage of the control. Any significant increase in LDH levels would indicate cellular disruption or death due to the treatment.

2.3.4. Statistical Analysis. For statistical analysis, all data are expressed as mean \pm standard deviation (SD). The graphs and curves are done with SigmaPlot 12.0, Adobe Photoshop 7.0, and Microsoft Office Excel 2007.

3. Results

In MTT assay only cells that are viable after 24 hours exposed to the sample were capable of metabolizing a dye (3-(4,5-dimethylthiazol-2-yl)-2,5-diphenyl tetrazolium bromide) efficiently and the purple colored precipitate which

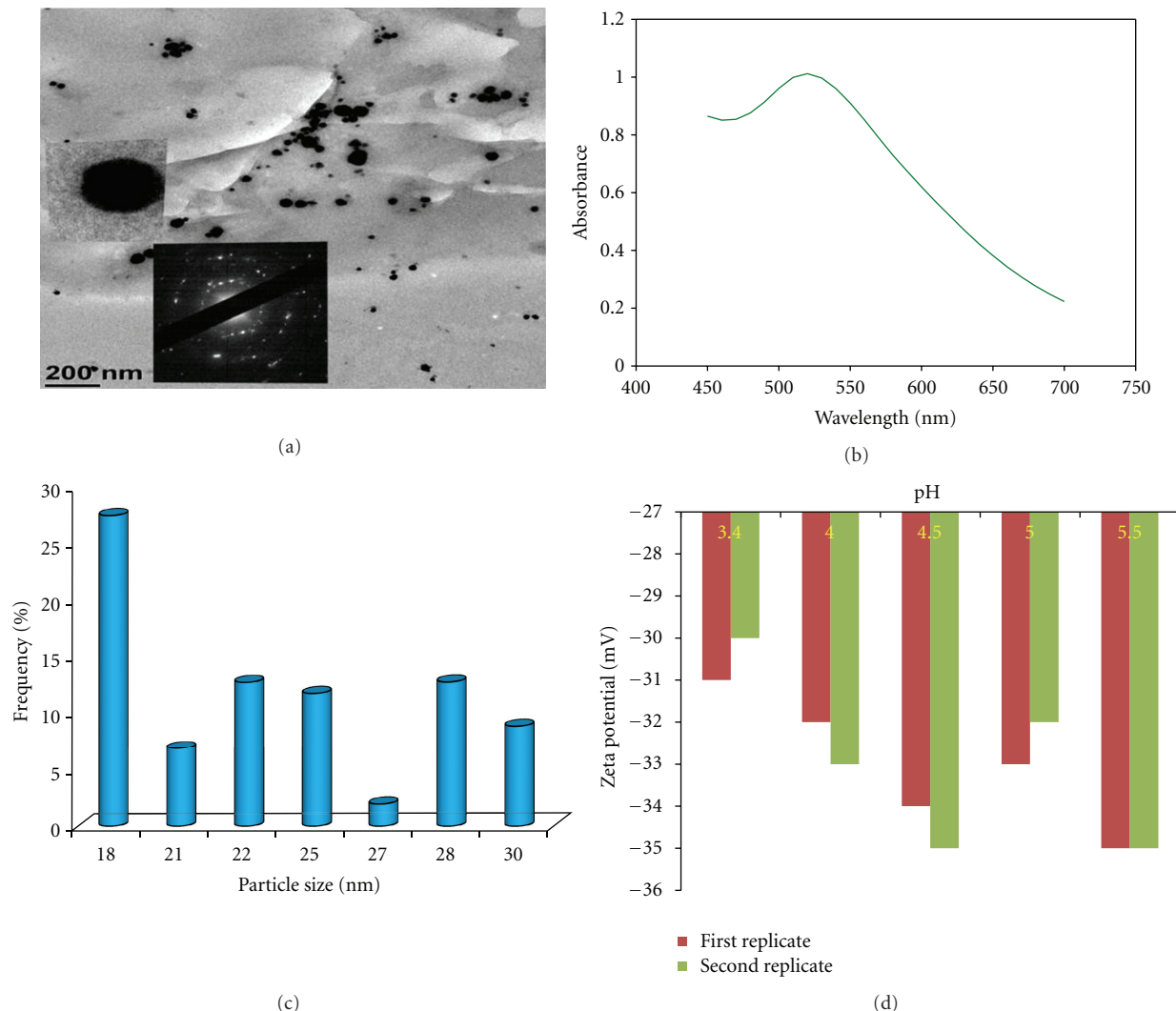


FIGURE 3: (a) TEM image of gum arabic stabilized gold nanoparticles. Insight SEAD pattern and an enlarged single nanoparticle. (b) Particle size histogram and is 20 nm averaged from 100 nanoparticles. (c) Plasmon resonance absorption and is 528 nm with plasmon width ($\Delta\lambda$) of 85 nm. (d) Zeta potential of gold nanoparticles at different pH values.

is dissolved in a detergent was analyzed spectrophotometrically. After 24 hours of posttreatment, PC-3 and MCF-7 cells showed excellent viability even up to the concentration of 140 μ g of citrate-, starch-, and gum arabic-capped gold nanoparticles. These results clearly demonstrate that the photochemicals within these herbs provide nontoxic coating on AuNPs and corroborate the results of the internalization studies discussed above. The lack of any noticeable toxicity of starch and gum arabic stabilized gold nanoparticles provide new opportunities for the safe application in molecular imaging and therapy. But the data shows that there is a marginal cytotoxic effect of citrate stabilized gold nanoparticles with the cell lines used.

The mammalian Chinese hamster ovary (CHO22) cell line was used in the elucidation of cytotoxicity effects of the selected gold nanoparticles by neutral red assay. This cell line has been termed as the mammalian equivalent of the model bacterium *E. coli* [32]. For the elucidation of the cytotoxicity of the gold nanoparticles, the CHO22 cells were treated with

the nanomaterials for 24 hours. The gold nanoparticles were investigated at five concentrations. The spectrophotometric measurements were done for the neutral red dye uptake and release. The viability assay data for the comparison is presented in the Figures 4(a), 4(b), and 4(c).

4. Discussion

Comparison of the stabilizing agents revealed that citrate produced more pronounced response and sensitivity to the dose changes and time assay. The higher dosage shows less viability of citrate stabilized nanoparticles than starch and gum arabic stabilized gold nanoparticles. Cell viability was also determined by an LDH release assay which was employed to measure the cytotoxicity of the gold nanoparticles at different concentrations. Damaged cells release cytoplasmic LDH, which catalyzes a conversion of tetrazolium salt to formazan.

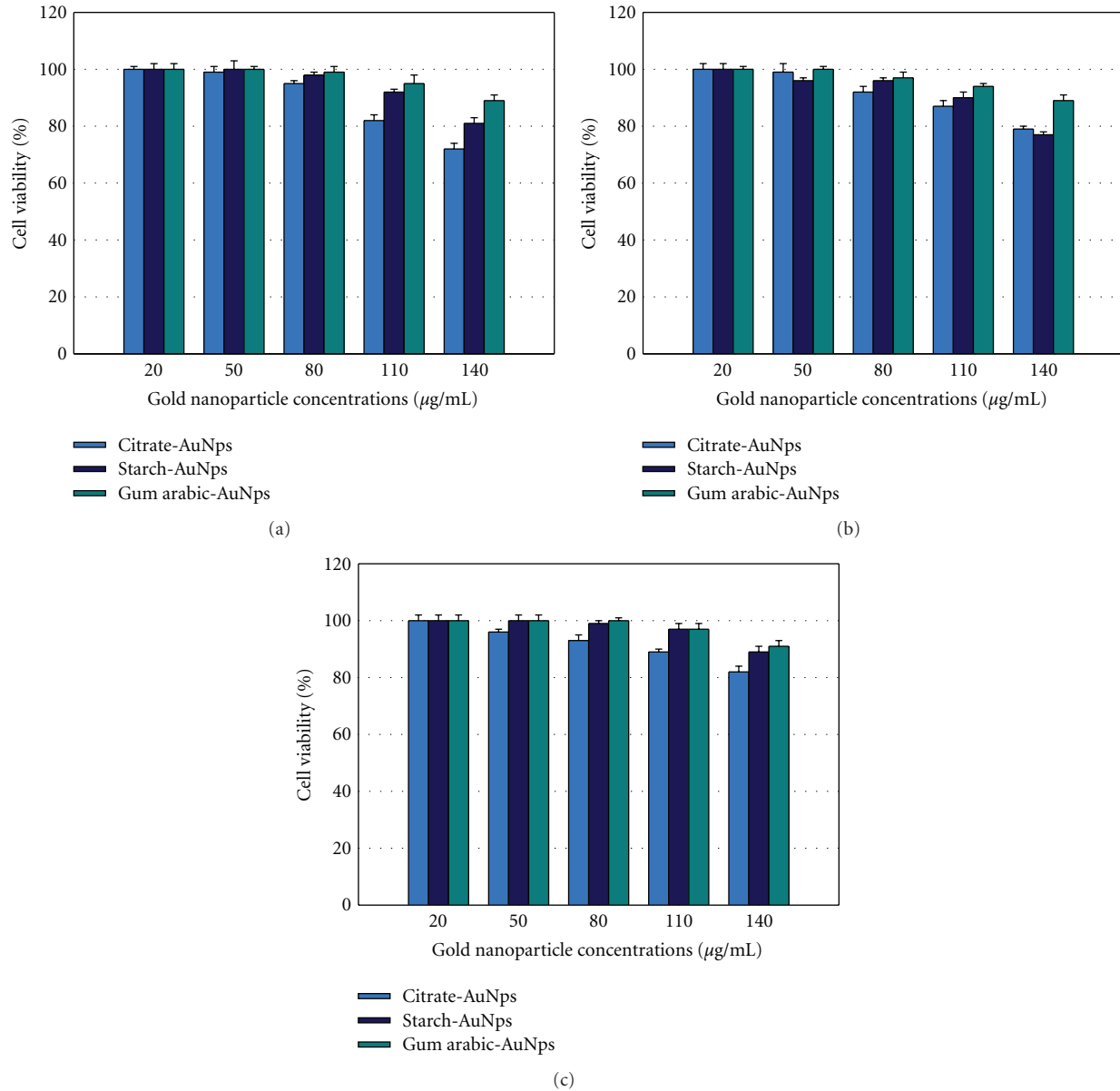


FIGURE 4: Cytotoxic assays by (a) MTT assay, (b) neutral red cell assay, and (c) LDH assay on gold nanoparticles stabilized with citrate, starch and gum arabic.

The absorbance of the produced formazan at 490 nm is proportional to the number of damaged or dying cells. The cytotoxicity of various cells in percent of LDH activity of the control, after exposure to increasing concentrations of nanoparticles stabilized with three different stabilizing agents for 24 hours, was analyzed. At each concentration, there was no significant cytotoxicity effect produced. The cell viability results indicate that gold nanoparticles are nontoxic to the array of cells tested. The incorporation of surface functionalities via citrate, starch, and gum arabic renders these nanoparticles highly biocompatible. Noble metal particles, such as gold are generally nontoxic due to their inert nature, this has also been seen with their LD_{50} in toxicity assays, high enough up to 1 mg/mL [33]. The

cell survival at different concentrations of gold nanoparticles stabilized with different capping agents showed a small variation with the increase in the concentration of the nanoparticles.

The gold nanoparticles of 20 nm are coated with citrate (citrate-AuNps), starch (starch-AuNps), and gum arabic (gum arabic-AuNps) are taken with a series of increasing concentrations (20, 50, 80, 110, and 140 $\mu\text{g}/\text{mL}$) along with cell cultures and studied under different cytotoxicity assays like MTT, neutral red cell, and LDH. In all the assays, the nanoparticles show excellent cell viability. The citrate stabilized gold nanoparticles rapidly show their cytotoxicity effect compared to starch and gum arabic. The gum arabic is highly viable than starch and citrate. In our observations,

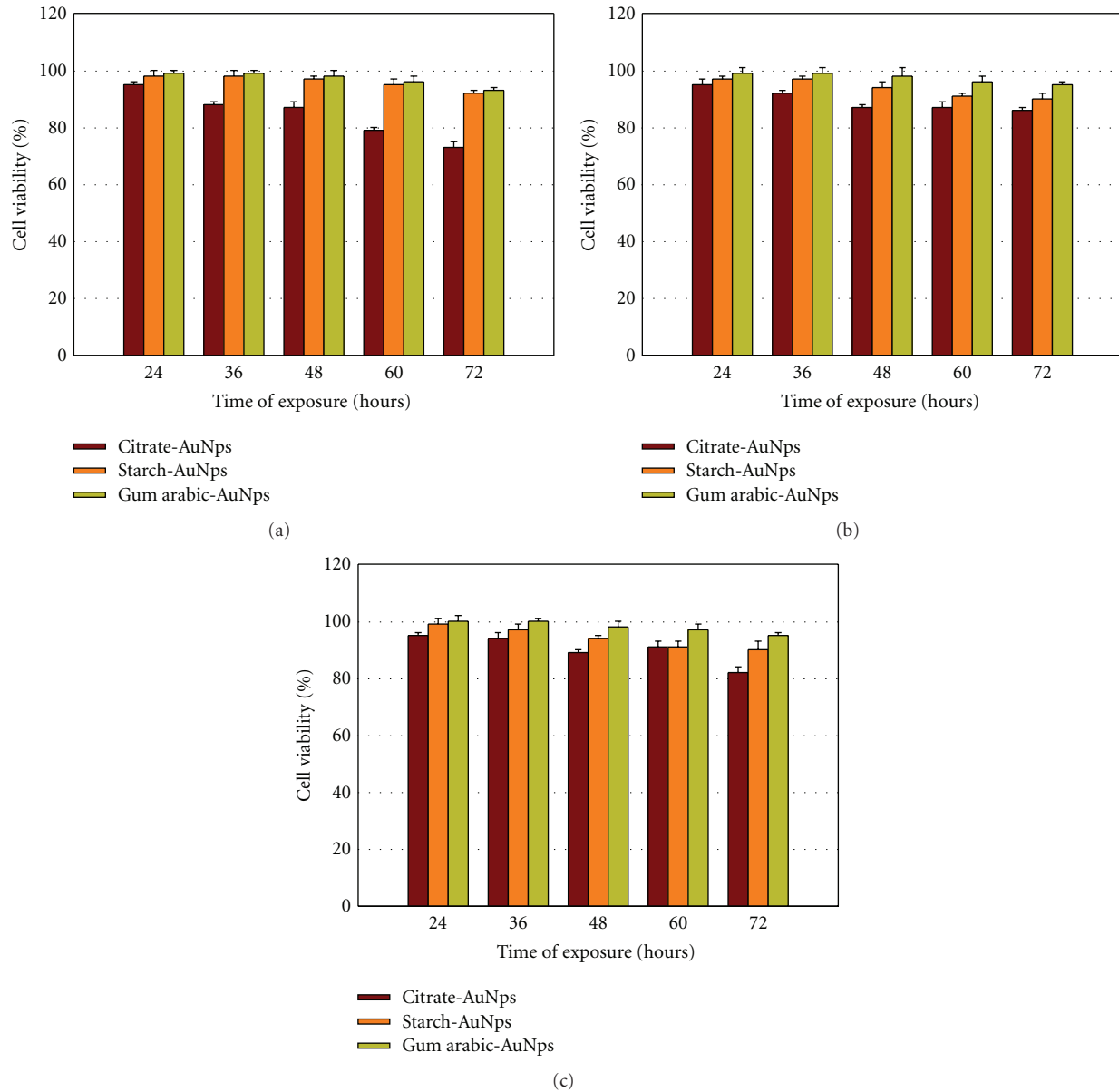


FIGURE 5: Cell viability studies at different time of exposure of citrate, starch, and gum arabic stabilized gold nanoparticles at a concentration of $110 \mu\text{g/mL}$ by (a) MTT assay, (b) neutral red cell assay, and (c) LDH assay.

all the gold nanoparticles are viable to cells and because of the acidic nature of citrate show little less cell viability compared to other stabilizing agents with gold nanoparticles. The viability test based on the time of exposure of gold nanoparticles was also studied with different stabilizing agents at different cell assays, Figures 5(a), 5(b), and 5(c). In this study the starch-AuNPs and gum arabic-AuNPs show high viability to cell assays compared to citrate-AuNPs, Figures 6(a), 6(b), and 6(c). IC_{50} is calculated as $110 \mu\text{g/mL}$ of gold nanoparticles and this concentration is considered for the time of exposure assay.

Cell-based cytotoxic assay with different concentrations of gold nanoparticles shows very small variation among citrate, starch, and gum arabic. The gold nanoparticles used

here were having the same size $20 \pm 1 \text{ nm}$, they differs only in stabilizing agents. The citrate stabilized gold nanoparticles show less viability than starch and gum arabic, Figures 4(a), 4(b), and 4(c). This is mainly due to the fact that citrate is acidic in nature. More over the particle sizes are same in all three cases of citrate, starch and gum arabic. Hence in this study the size dependent cytotoxicity is ruled out and it is confirmed that the stabilizing agents are responsible for cytotoxicity.

These results are consistent with previous investigations performed with dermal fibroblasts [34] which demonstrated that the gold/citrate nanoparticles impaired the proliferation of dermal fibroblasts and induced an abnormal formation of actin filaments, causing therefore a reduced cellular

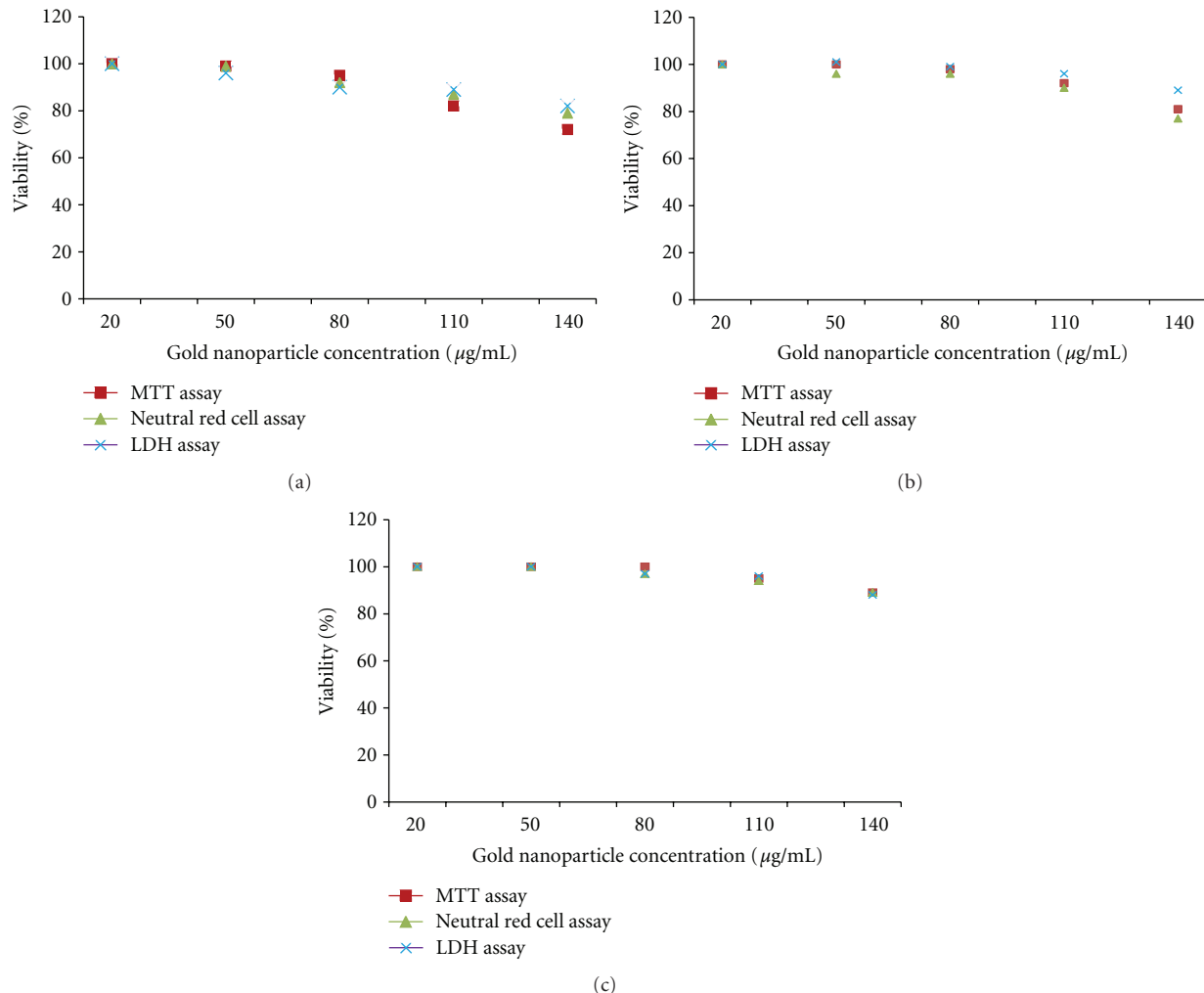


FIGURE 6: Different cell viability assays at different concentrations of gold nanoparticles for (a) citrate-capped (b) starch-capped, and (c) gum arabic capped.

motility and influencing the cell morphology. On contrary, [35] reported that citrated and biotinylated 18 nm gold nanoparticles did not induce toxicity in leukemic cells (cell line K562), whereas smaller particles were much more toxic.

5. Conclusion

In conclusion, we found that the gold nanoparticles stabilized with citrate, starch, and gum arabic are viable to different cells through different assays and with different concentrations of gold nanoparticles. The viability of the treated cells depending on the stabilizing agent and the types of cytotoxicity assay used. The cell viability test shows distinguishable cytotoxic effect for citrate stabilized gold nanoparticles at higher concentration and this is may be because the surface coating is acidic in nature compared to starch and gum arabic.

References

- [1] A. P. Alivisatos, "Semiconductor clusters, nanocrystals, and quantum dots," *Science*, vol. 271, no. 5251, pp. 933–937, 1996.

- [2] D. L. Feldheim, A. F. Colby, and D. Marcel : , "Metal nanoparticles: synthesis, characterization and applications," *The Journal of Physical Chemistry*, vol. 300, pp. 11202–11208, 2002.
- [3] D. V. Leff, L. Brandt, and J. R. Heath, "Synthesis and characterization of hydrophobic, organically-soluble gold nanocrystals functionalized with primary amines," *Langmuir*, vol. 12, no. 20, pp. 4723–4730, 1996.
- [4] C. M. Niemeyer, "Nanoparticles, proteins, and nucleic acids: biotechnology meets materials science," *Angewandte Chemie—International Edition*, vol. 40, no. 22, pp. 4129–4158, 2001.
- [5] J. C. Sanford, F. D. Smith, and J. A. Russell, "Optimizing the biolistic process for different biological applications," *Methods in Enzymology*, vol. 217, pp. 483–509, 1993.
- [6] A. Bielinska, J. D. Eichman, I. Lee, J. R. Baker, and L. Balogh, "Imaging Au0-PAMAM gold-dendrimer nanocomposites in cells," *Journal of Nanoparticle Research*, vol. 4, no. 5, pp. 395–403, 2002.
- [7] L. Olofsson, T. Rindzevicius, I. Pfeiffer, M. Käll, and F. Höök, "Surface based Gold nanoparticle sensor for specific and quantitative DNAHybridization detection," *Langmuir*, vol. 19, no. 24, pp. 10414–10419, 2003.

- [8] P. Zrazhevskiy, M. Sena, and X. Gao, "Designing multifunctional quantum dots for bioimaging, detection, and drug delivery," *Chemical Society Reviews*, vol. 39, no. 11, pp. 4326–4354, 2010.
- [9] J. H. Lee, Y. M. Huh, Y. W. Jun et al., "Artificially engineered magnetic nanoparticles for ultra-sensitive molecular imaging," *Nature Medicine*, vol. 13, no. 1, pp. 95–99, 2007.
- [10] C. R. Thomas, D. P. Ferris, J. H. Lee et al., "Noninvasive remote-controlled release of drug molecules *in vitro* using magnetic actuation of mechanized nanoparticles," *Journal of the American Chemical Society*, vol. 132, no. 31, pp. 10623–10625, 2010.
- [11] T. Neuberger, B. Schöpf, H. Hofmann, M. Hofmann, and B. Von Rechenberg, "Superparamagnetic nanoparticles for biomedical applications: possibilities and limitations of a new drug delivery system," *Journal of Magnetism and Magnetic Materials*, vol. 293, no. 1, pp. 483–496, 2005.
- [12] X. Qian, X. H. Peng, D. O. Ansari et al., "*In vivo* tumor targeting and spectroscopic detection with surface-enhanced Raman nanoparticle tags," *Nature Biotechnology*, vol. 26, no. 1, pp. 83–90, 2008.
- [13] X. Bai, S. J. Son, S. Zhang et al., "Synthesis of superparamagnetic nanotubes as MRI contrast agents and for cell labeling," *Nanomedicine*, vol. 3, no. 2, pp. 163–174, 2008.
- [14] S. J. Son, X. Bai, and S. B. Lee, "Inorganic hollow nanoparticles and nanotubes in nanomedicine. Part 1. Drug/gene delivery applications," *Drug Discovery Today*, vol. 12, no. 15–16, pp. 650–656, 2007.
- [15] S. J. Son, J. Reichel, B. He, M. Schuchman, and S. B. Lee, "Magnetic nanotubes for magnetic-field-assisted bioseparation, biointeraction, and drug delivery," *Journal of the American Chemical Society*, vol. 127, no. 20, pp. 7316–7317, 2005.
- [16] D. T. Mitchell, S. B. Lee, L. Trofin et al., "Smart nanotubes for bioseparations and biocatalysis," *Journal of the American Chemical Society*, vol. 124, no. 40, pp. 11864–11865, 2002.
- [17] B. He, S. K. Kim, S. J. Son, and S. B. Lee, "Shape-coded silica nanotubes for multiplexed bioassay: rapid and reliable magnetic decoding protocols," *Nanomedicine*, vol. 5, no. 1, pp. 77–88, 2010.
- [18] C. Kirchner, T. Liedl, S. Kudera et al., "Cytotoxicity of colloidal CdSe and CdSe/ZnS nanoparticles," *Nano Letters*, vol. 5, no. 2, pp. 331–338, 2005.
- [19] R. A. Goyer, "Nutrition and metal toxicity," *American Journal of Clinical Nutrition*, vol. 61, no. 3, supplement, pp. 646S–650S, 1995.
- [20] L. Ghitescu and A. Fixman, "Surface charge distribution on the endothelial cell of liver sinusoids," *Journal of Cell Biology*, vol. 99, no. 2, pp. 639–647, 1984.
- [21] W. J. Parak, R. Boudreau, M. Le Gros et al., "Cell motility and metastatic potential studies based on quantum dot imaging of phagokinetic tracks," *Advanced Materials*, vol. 14, no. 12, pp. 882–885, 2002.
- [22] X. Li, C. A. van Blitterswijk, Q. Feng, F. Cui, and F. Watari, "The effect of calcium phosphate microstructure on bone-related cells *in vitro*," *Biomaterials*, vol. 29, no. 23, pp. 3306–3316, 2008.
- [23] X. Li, H. Liu, X. Niu et al., "The use of carbon nanotubes to induce osteogenic differentiation of human adipose-derived MSCs *in vitro* and ectopic bone formation *in vivo*," *Biomaterials*, vol. 33, no. 19, pp. 4818–4827, 2012.
- [24] D. B. Warheit, B. R. Laurence, K. L. Reed, D. H. Roach, G. A. M. Reynolds, and T. R. Webb, "Comparative pulmonary toxicity assessment of single-wall carbon nanotubes in rats," *Toxicological Sciences*, vol. 77, no. 1, pp. 117–125, 2004.
- [25] R. Judson, A. Richard, D. J. Dix et al., "The toxicity data landscape for environmental chemicals," *Environmental Health Perspectives*, vol. 117, no. 5, pp. 685–695, 2009.
- [26] R. Shukla, V. Bansal, M. Chaudhary, A. Basu, R. R. Bhonde, and M. Sastry, "Biocompatibility of gold nanoparticles and their endocytotic fate inside the cellular compartment: a microscopic overview," *Langmuir*, vol. 21, no. 23, pp. 10644–10654, 2005.
- [27] J. Turkevich, P. C. Stevenson, and J. Hillier, "A study of the nucleation and growth processes in the synthesis of colloidal gold," *Discussions of the Faraday Society*, vol. 11, pp. 55–75, 1951.
- [28] J. Kimling, M. Maier, B. Okenve, V. Kotaidis, H. Ballot, and A. Plech, "Turkevich method for gold nanoparticle synthesis revisited," *Journal of Physical Chemistry B*, vol. 110, no. 32, pp. 15700–15707, 2006.
- [29] G. Frens, "Particle size and sol stability in metal colloids," *Kolloid-Zeitschrift & Zeitschrift für Polymere*, vol. 250, no. 7, pp. 736–741, 1972.
- [30] K. Aika, L. T. Ban, I. Okura et al., "Journal of the Research Institute of Catalysis," *Hokkaido University*, vol. 24, no. 1, pp. 54–64, 1976.
- [31] T. Mosmann, "Rapid colorimetric assay for cellular growth and survival: application to proliferation and cytotoxicity assays," *Journal of Immunological Methods*, vol. 65, no. 1–2, pp. 55–63, 1983.
- [32] F. T. Kao and T. T. Puck, "Genetics of somatic mammalian cells, VII. Induction and isolation of nutritional mutants in Chinese hamster cells," *Proceedings of the National Academy of Sciences of the United States of America*, vol. 60, no. 4, pp. 1275–1281, 1968.
- [33] Z. P. Xu, Q. H. Zeng, G. Q. Lu, and A. B. Yu, "Inorganic nanoparticles as carriers for efficient cellular delivery," *Chemical Engineering Science*, vol. 61, no. 3, pp. 1027–1040, 2006.
- [34] N. Pernodet, X. Fang, Y. Sun et al., "Adverse effects of citrate/gold nanoparticles on human dermal fibroblasts," *Small*, vol. 2, no. 6, pp. 766–773, 2006.
- [35] E. E. Connor, J. Mwamuka, A. Gole, C. J. Murphy, and M. D. Wyatt, "Gold nanoparticles are taken up by human cells but do not cause acute cytotoxicity," *Small*, vol. 1, no. 3, pp. 325–327, 2005.



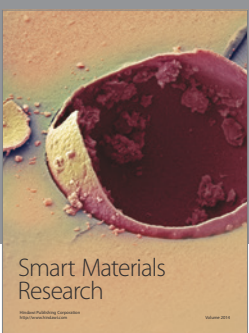
Journal of
Nanotechnology



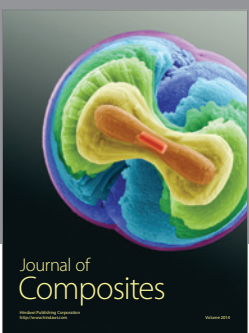
International Journal of
Corrosion



International Journal of
Polymer Science



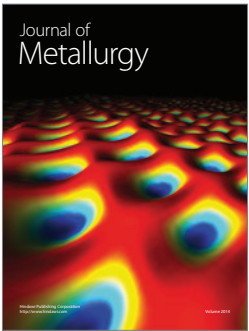
Smart Materials
Research



Journal of
Composites



BioMed
Research International



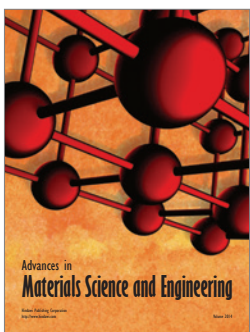
Journal of
Metallurgy



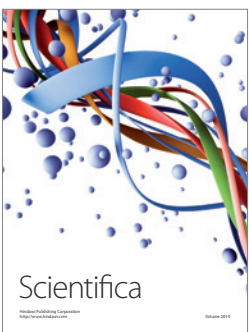
Journal of
Materials



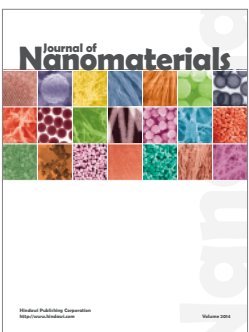
Journal of
Nanoparticles



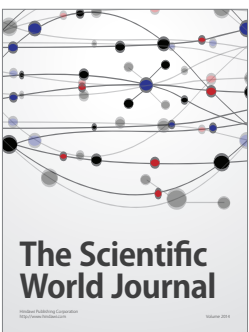
Advances in
Materials Science and Engineering



Scientifica



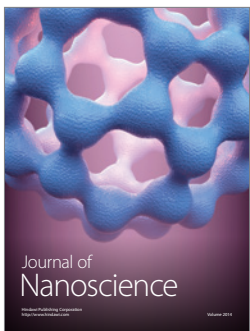
Journal of
Nanomaterials



The Scientific
World Journal



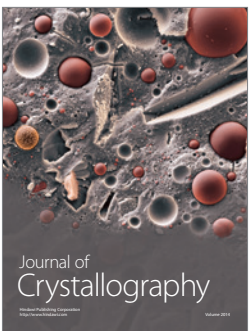
International Journal of
Biomaterials



Journal of
Nanoscience



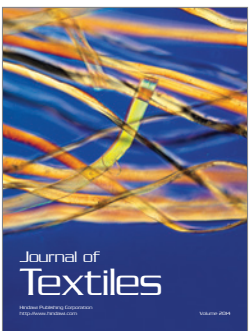
Journal of
Coatings



Journal of
Crystallography



Journal of
Ceramics



Journal of
Textiles